Nanoscale Advances

ROYAL SOCIETY OF CHEMISTRY

PAPER

View Article Online
View Journal | View Issue

Cite this: *Nanoscale Adv.*, 2021, **3**, 6965

Eco-friendly and facile synthesis of size-controlled spherical silica particles from rice husk†

Seongseop Kim, ‡[a] Ji Yeon Park,[bc] Yang Mo Gu,[bc] Il-Seop Jang,[de] Hayoung Park,[de] Kyeong Keun Oh,[f] Jin Hyung Lee*[b] and Jinyoung Chun*[d]

The valorization of inorganic silica components from rice husk has been considered an important research topic over the last few decades. However, owing to various problems, such as the difficulty in controlling precise morphological properties, complex extraction and manufacturing processes, and the use of hazardous acids, the technology for producing high value-added silica for industrial applications is still insufficient. In this study, we developed a method for obtaining size-controlled spherical silica from rice husk using an eco-friendly and simplified process that overcomes the above-mentioned limitations. Silica particles were obtained by extraction from rice husk in alkaline media under mild conditions (80 °C) followed by pH adjustment with acetic acid. Therefore, the use of strong acids was excluded, no special equipment was required for the process, and the overall synthetic process was significantly simplified. The silica particles obtained through this method were uniformly spherical in shape, with a surface area of more than 200 $m^2\ g^{-1}$. Our results indicate that the preparation of silicate solution under appropriate conditions and the use of polyethylene glycol (PEG) additives during the precipitation step are important for obtaining spherical silica. Moreover, by adjusting the temperature in the precipitation step, the size of the spherical silica particles can be controlled in the range of ~250 nm to ~1.4 μm. Our study contributes to the development of rice husk-derived silica that can be applied to practical industrial applications.

Received 7th September 2021
Accepted 7th October 2021

DOI: 10.1039/d1na00668a

rsc.li/nanoscale-advances

Introduction

Rice husk, a residue from the rice milling process, is one of the most produced biomass materials in the world. The Food and Agricultural Organization (FAO) reported a global rice production of 996 million tons in 2018.[1] This statistic indicates that approximately 200 million tons of rice husk were produced in a single year, as rice husk accounts for approximately 20% of produced rice. Therefore, the effective treatment of rice husk and its conversion into a high value-added material are very important topics for research. Notably, the average content of silica (SiO_2) in rice husk lies at 10.6%, which represents the highest ratio of silica components among different biomaterials.[2] This means that rice husk can be an environmentally friendly and inexpensive source of silica, and thus, many researchers have focused on the utilization of silica from rice husk.[3,4]

The widely adopted approach for obtaining inorganic silica from rice husk is through direct combustion. This is a simple and cost-effective process, which can control the surface area, purity, and crystallinity of silica by adjusting the combustion conditions.[5,6] Chemical treatments, such as acid leaching, have also been investigated to obtain high-purity silica with a large surface area from rice husk.[7–10] For example, it was reported that silica particles with a purity of more than 99.5% could be successfully obtained through acid leaching followed by pyrolysis, with a surface area of 85 $m^2\ g^{-1}$.[9] Vayghan *et al.* reported that silica particles with a purity of 98% were obtained from pre-combustion acid-treated rice husk; the particles had a surface area of more than 280 $m^2\ g^{-1}$.[8] However, these methods not only result in the release of greenhouse gases or rely on the use of strong acids but also have clear limitations in terms of the shape and porous structure of the silica products.[11,12] Although research on producing silica with a high purity and surface area

[a]*Max-Planck-Institut für Kohlenforschung, Kaiser-Wilhelm-Platz 1, Mülheim an der Ruhr, 45470, Germany*

[b]*Convergence R&D Division, Korea Institute of Ceramic Engineering and Technology (KICET), Cheongju, Chungbuk 28160, Republic of Korea. E-mail: leejinh1@kicet.re.kr*

[c]*Division of Chemical Engineering & Bio Engineering, Hanyang University, Seoul, 04763, Republic of Korea*

[d]*Energy and Environment Division, Korea Institute of Ceramic Engineering and Technology (KICET), Jinju, Gyeongnam 52851, Republic of Korea. E-mail: jchun@kicet.re.kr*

[e]*Department of Materials Science and Engineering, Korea University, Seoul 02841, Republic of Korea*

[f]*Department of Chemical Engineering, Dankook University, Yongin, Gyeonggi 16890, Republic of Korea*

† Electronic supplementary information (ESI) available. See DOI: 10.1039/d1na00668a

‡ Current address: School of Chemical Engineering, Jeonbuk National University, Jeonju 54896, Republic of Korea.

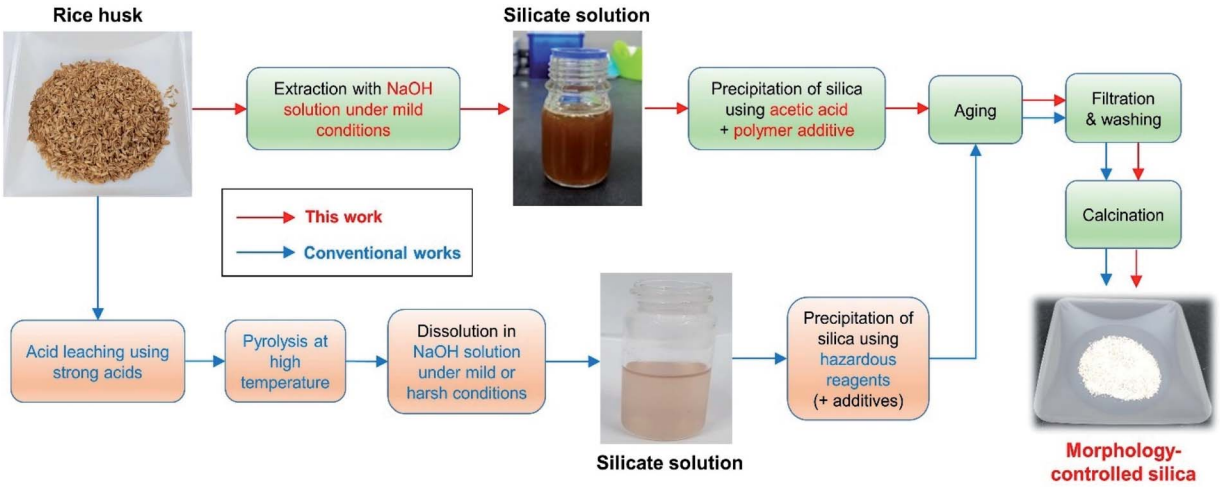

Fig. 1 Schematic representation of the procedure used to obtain morphology-controlled silica particles from rice husk.

through an eco-friendly process in which strong acids are replaced with an ionic liquid has been published, some limitations still exist in terms of precise morphology control of silica and the need for very expensive reagents.[9]

To obtain the high value-added silica required for various applications in modern industries, including the cosmetics, catalyst, biomaterial, and energy device industries,[13–19] it is essential that the silica particles derived from rice husk have precise and specific morphological properties. Accordingly, synthetic methods based on bottom-up processes, which obtain nano- or micro-particles through chemical reactions of precursors at the atomic or molecular level, have received increasing research interest over recent years.[12] In particular, various studies have investigated the production of nanostructured silica with well-defined mesopores through bottom-up processes using a rice husk-derived silicate solution.[4,20–28]

However, some critical problems are yet to be solved, including the following: (i) synthetic methods are complex; the steps include the acid leaching of rice husk, pyrolysis, silicate extraction in alkaline media, and reprecipitation with hazardous reagents (*e.g.*, ammonia, sulfuric acid, and hydrochloric acid) (Fig. 1). The acid leaching of rice husk usually relies on the use of strong acids. Alkali extraction sometimes progresses at temperatures above the boiling point of the solution,[4,21,25,28] in which case the evaporation of the solvent has to be safely prevented. This results in large energy consumption, and an increase in the process cost due to multiple steps and special equipment. This makes it difficult to apply the developed methods to real industries; (ii) although most studies have focused on controlling the pore structure and surface area of produced silica, there is a lack of research centered on the shape of silica particles; (iii) although several studies have reported on the production of spherical silica particles from rice husk, results included an uneven size distribution or aggregation of particles, and high-risk acids were still required during the acid leaching or precipitation steps.[29–33] Therefore, to obtain high value-added silica from rice husk through precise morphological control for use in real industries, the above-mentioned problems must be solved comprehensively.

In this study, we developed and investigated an eco-friendly and facile method for obtaining size-controlled spherical silica particles from rice husk. Specifically, we obtained silica particles by alkali extraction under mild conditions, followed by precipitation with acetic acid (Fig. 1). Therefore, the use of strong acids was excluded, no special equipment was required, and the overall synthetic process was simplified. The silica particles obtained through this method were uniformly spherical in shape with a large surface area. Our results indicate that the preparation of silicate solution under appropriate conditions and the use of polyethylene glycol (PEG) additives during the precipitation step are important for obtaining spherical silica particles. As PEG has a sufficient number of ethylene oxide (EO) chains to stabilize the silicate species, it is presumed that even a small amount of PEG additive can control the morphology of the silica particles. PEG also has the advantageous of low toxicity and low cost, meaning that the manufacturing process can be made cheaper and safer. Furthermore, by adjusting the reaction temperature during precipitation, the size of the silica particles could be controlled in the range of ~250 nm to ~1.4 μm. Thus, we expect the developed method to have a great impact on the production of rice husk-derived silica for use in the practical industrial applications.

Results and discussion

Extraction of silica from rice husks

Initially, the effect of the NaOH concentration on the silica extraction yield from rice husk was investigated. Five concentrations of NaOH, 0.1, 0.15, 0.2, 0.5, and 1.0 M, were used to extract silica from rice husk at 80 °C. As shown in Fig. 2a, the use of 0.1 M NaOH could extract a small quantity of silica from rice husk, only 1%. After increasing to only 0.15 M concentration, silica extraction increased to 73%. Over 0.2 M NaOH, the

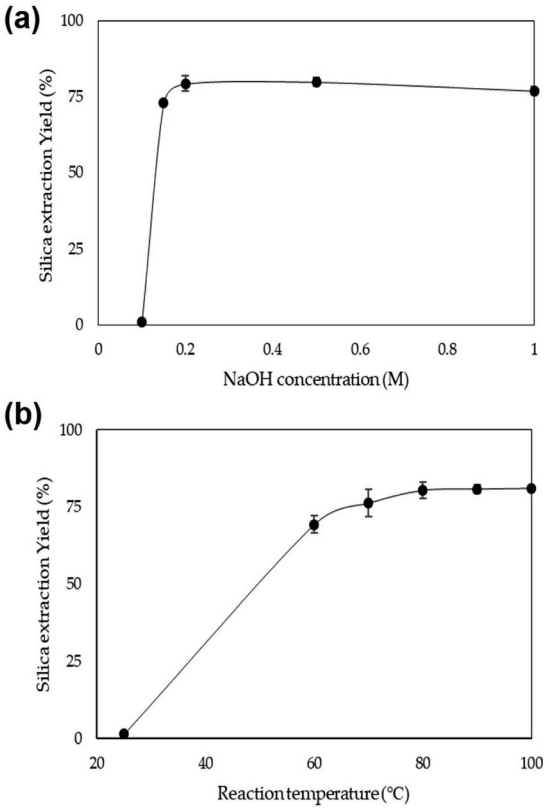

Fig. 2 Silica extraction yield depending on (a) the NaOH concentration at 80 °C and (b) the temperature using 0.2 M NaOH.

silica extraction yield was consistent at around 80%. In this experiment, the solid content in the NaOH leaching solution was 6 wt%. Therefore, 0.13 g-NaOH/g-rice husk was enough to extract silica from rice husk. The reaction temperature was investigated to find optimum reaction conditions when 0.2 M NaOH was used to extract silica (Fig. 2b). The reaction temperature of 25 °C was too low to extract silica from rice husk effectively, with only 1.4% silica yield. With increasing temperature, silica extraction yields increased up to 80 °C. The silica extraction yields at 80 °C were around 80%. However, the silica extraction yield did not significantly increase even as the temperature increased up to 100 °C. These results show that sufficient silica can be extracted from rice husk even under mild conditions, low NaOH concentration and low reaction temperature below 100 °C.

The rice husk used in this study was composed of 52 wt% carbohydrates, 29 wt% lignin, and 14 wt% ash (Table 1). After treating with 0.2 M NaOH solution at 80 °C, the composition of the extracted solution was 46 wt% ash, 23 wt% lignin, and 19 wt% carbohydrates (Table 1). This result shows that some carbohydrates and lignin in rice husk were also leached into the solution, 9% and 19%, respectively. However, we found that if the ratio of leached carbohydrates and lignin is not relatively high, it does not interfere with the morphology control of silica particles, which are synthesized using the extracted solution in the next process. This will be further discussed in the next section.

On the other hand, when silica in rice husk was extracted under harsh conditions (150 °C), a large amount of carbohydrates and lignin was also leached into the solution. The composition of the extracted solution under harsh conditions was 31 wt% ash, 36 wt% lignin, and 24 wt% carbohydrates (Table 1). This indicates that almost 21% of carbohydrates and 56% of lignin in rice husk were leached into the solution. Accordingly, although the silica extraction yields under harsh conditions slightly increased due to high temperature and pressure (Fig. S1†), morphology-controlled silica particles could not be obtained in the next process due to the large amounts of organic components in the extracted solution. The effect of the extraction conditions on the production of silica particles will be covered in the next section.

Synthesis of spherical silica particles from rice husk-derived silicate solution

Uniformly spherical silica particles were synthesized using a silicate solution extracted from rice husk under mild conditions (80 °C). To reduce the risk and related environmental hazards, acetic acid was used in place of a strong acid during precipitation. The overall synthetic process is summarized in Fig. 1, and the detailed procedures are described in the Experimental section. Spherical silica particles obtained by adjusting the pH of the silicate solution at room temperature (25 °C) were denoted as SS-1. The scanning electron microscopy (SEM) and transmission electron microscopy (TEM) images of SS-1 showed the formation of uniformly spherical particles (Fig. 3a–c), with the particle size distribution indicating an average particle size of approximately 800 nm (Fig. 3d). The X-ray diffraction (XRD)

Table 1 Compositions of raw rice husk and NaOH-treated rice husk[a]

	Carbohydrates (wt%)	Lignin (wt%)	Ash[b] (wt%)	Others (wt%)
Raw rice husk	52	29	14	5
Extracted silicate solution (80 °C)	19	23	46	12
Residual solid (80 °C)	62	31	3	4
Extracted silicate Solution (150 °C)	24	36	31	9
Residual solid (150 °C)	88	12	—	—

[a] Ash means inorganic solid components. [b] See Tables 2 and S1 for the silica content in the ash.

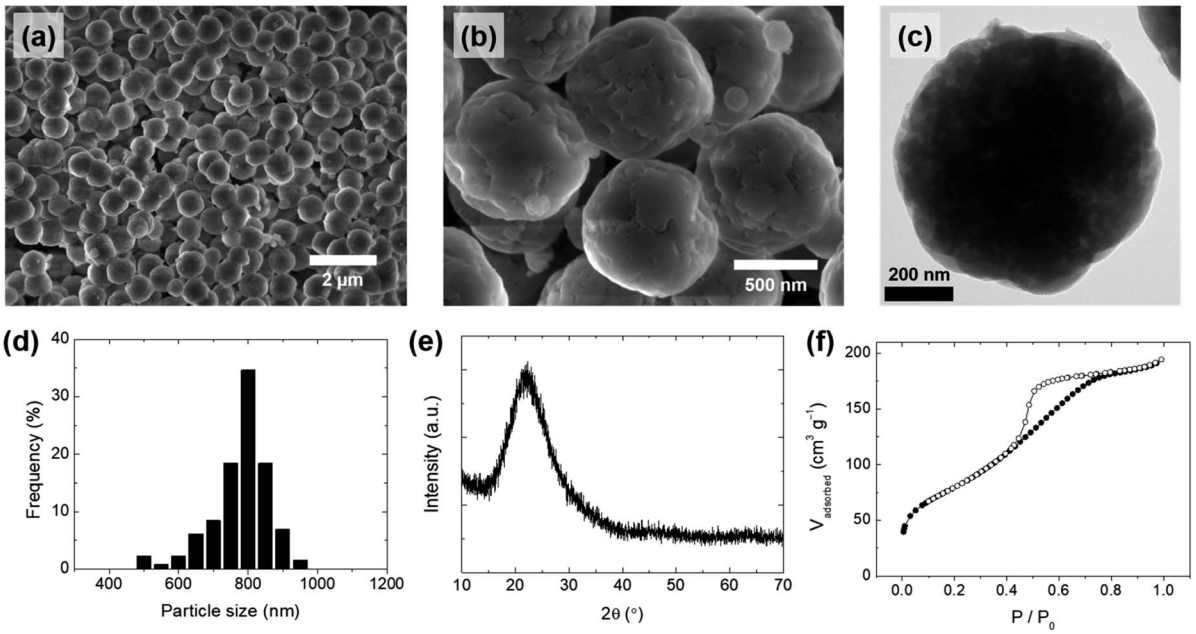

Fig. 3 (a and b) Scanning electron microscopy (SEM) images, (c) transmission electron microscopy (TEM) image, (d) particle size distribution, (e) X-ray diffraction (XRD) pattern, and (f) nitrogen (N_2) physisorption isotherms of spherical silica particles (SS-1), obtained by precipitation at room temperature (25 °C).

pattern of SS-1 only exhibited a broad peak at around 22°, which is typical of amorphous silica (Fig. 3e). The porous structure of SS-1 was generated by removing organic components. PEG molecules were confined in the silica to stabilize silicates during precipitation. After washing and calcination, the space occupied by PEG molecules and lignin was converted into pores. The pore size distribution calculated from the adsorption branch of the nitrogen (N_2) physisorption isotherms showed a main pore size of ~4 nm (Fig. 3f and S2a†). SS-1 had a large surface area of 291 $m^2\ g^{-1}$, owing to the presence of micropores with mesopores on the silica particles. The silica purity of SS-1 was 97.76%, as determined by inductively coupled plasma-optical emission spectroscopy (ICP-OES) analysis (Table 2). In addition, no hazardous elements such as heavy metals were detected. Residual carbon components originating from lignin or the PEG additive were successfully removed by calcination at 550 °C (Table 2). Finally, approximately 0.1 g of SS-1 was obtained per 1 g of rice husk; the silica production yield from the silicate solution was ~93% (Fig. S3†). Additionally, our result showed that 2% of the sodium containing impurities could easily be removed by washing with a diluted acetic acid solution (see the ESI†). Notably, the purity of the spherical silica increased to 99.9% by additional washing (Table S1†). The overall analysis results confirmed the synthesis of uniformly spherical silica nanoparticles with high purity and a large surface area from the rice husk-derived silicate solution.

PEG plays an important role in the control of the particle morphology of silica during the precipitation. For comparison,

Table 2 Inorganic compositions and carbon content of SS-1, S-1, and S-2

	Components	SS-1	S-1	S-2
ICP-OES	SiO_2	97.76	98.15	97.85
	Na_2O	2.000	1.763	2.030
	Al_2O_3	0.017	0.011	0.018
	Fe_2O_3	0.017	0.003	0.002
	CaO	0.039	0.018	—
	MgO	0.057	0.007	—
	K_2O	0.067	0.046	0.097
	MnO	0.032	0.004	—
Elemental analysis	Carbon (after drying)	6.64	1.80	8.09
	Carbon (after calcination)	0.03	0.02	0.13

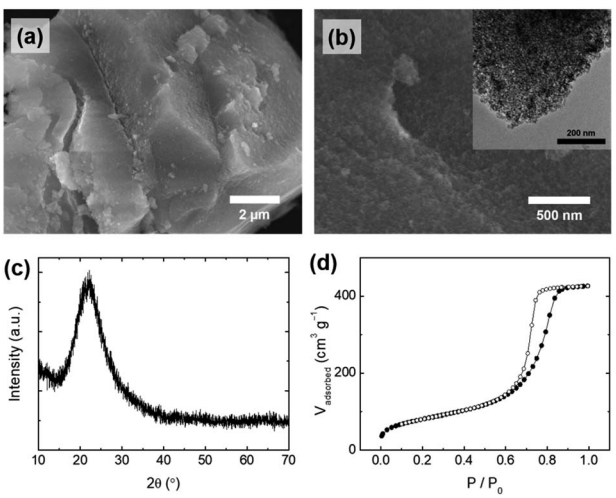

Fig. 4 (a and b) SEM images (inset: TEM image), (c) XRD pattern, and (d) N_2 physisorption isotherms of silica particles (S-1), synthesized without the polyethylene glycol (PEG) additive.

Table 3 Surface area, pore volume, average pore size, and average particle size of silica particles

	SS-1	SS-2	SS-3	SS-4	S-1	S-2
Silicate extraction conditions	Mild (80 °C)					Harsh (150 °C)
Precipitation temperature	25 °C	5 °C	40 °C	60 °C	25 °C	25 °C
Additive	PEG	PEG	PEG	PEG	None	PEG
Surface area ($m^2\ g^{-1}$)	291	221	328	407	294	294
Pore volume ($cm^3\ g^{-1}$)	0.301	0.131	0.381	0.659	0.659	1.19
Average pore size (nm)	4.13	2.38	4.64	6.48	8.98	16.1
Average particle size (nm)	789 (±81)	1355 (±290)	400 (±124)	250 (±71)	N/A	N/A

bulk silica particles (S-1) were prepared with an identical procedure to SS-1 in the absence of the PEG additive. Fig. 4a and b show the overall morphology of S-1; only large-sized particles with irregular shapes were observed in the microscope images of S-1, indicating that PEG is an essential additive for controlling the spherical shape of silica particles. Similar phenomena were observed in previous studies that produced spherical silica using polymer additives.[34,35] The silicate species were hydrolyzed and condensed for the silica growth, and therefore they have a number of hydroxyl groups, allowing interaction with EO chains in PEG by hydrogen bonding. When EO chains are long enough, the silicate species can be stabilized by interaction with EO chains during the precipitation process, leading to the formation of spherically shaped particles. As shown in Fig. S4,† absorption peaks related to the stretching and bending mode of the functional groups in PEG were also observed in the IR spectrum of SS-1 (before calcination). Referring to the results of previous studies,[34,35] we assumed that the molecular weight of the PEG polymer (M_r: 2700–3300) used in this study was sufficient to produce uniform spherical particles.

The pore properties (*e.g.*, pore size and pore volume) of S-1 were also changed in the absence of the PEG additive. The silicate species were precipitated with bulky organic components (*e.g.*, lignin) to form irregular particles. Mesopores of S-1 were generated by removing lignin molecules after calcination, which is different from the formation of mesopores of SS-1. Lignin is composed of phenolic macromolecules which are larger molecules than PEG, resulting in an increased pore size (~9 nm) and pore volume (0.659 $cm^3\ g^{-1}$) of S-1 compared to those of SS-1 (Fig. 4d, S2b† and Table 3). For these reasons, S-1 showed a very large difference in the particle shape and pore properties from those of SS-1, while the other physicochemical properties of S-1 are similar to those of SS-1: purity (98.15%, Table 1), surface area (294 $m^2\ g^{-1}$), and amorphous crystallinity (Fig. 4c). The concentration of PEG used when producing the silica particles also affects the uniformity of their shape. When less than 0.4 g of PEG per 200 mL of silicate solution was used, only irregular particles were obtained (data not shown). Therefore, we assumed that a certain concentration of PEG or higher is required to interact with the hydroxyl group of silica sufficiently for uniform spherical silica to form.

Interestingly, the conditions under which the silicate solution is extracted from the rice husk also affected the morphology of the silica particles obtained from the silicate solution. When the silicate solution was extracted under harsh conditions (150 °C), only irregularly shaped particles (S-2) were obtained (Fig. 5a and b). Even though PEG was added in the same way as in the preparation of the SS-1 sample, the morphology of the S-2 particles differed from that of the SS-1 particles. The silicate solution extracted under harsh conditions contained a relatively large amount of dissolved organic components compared to that extracted under mild conditions (80 °C). Although there is a difference in absolute values, both PEG and organic components (*e.g.*, lignin) are negatively charged at neutral pH. Accordingly, we suggest that the organic components hinder the interaction of PEG with silicate species, thereby reducing the effect of the addition of PEG. Therefore, S-2 particles exhibited an irregular shape similar to that of S-1, but not that of SS-1. The surface area of S-2 (294 $m^2\ g^{-1}$) was similar to that of S-1, but its pore volume (1.19 $cm^3\ g^{-1}$) and average pore size (~16 nm) were larger than those of S-1 (Fig. 5d, S2c† and Table 3). This tendency may also be affected by the presence of organic components. As a large amount of organic components that had assembled with the precipitated silica was removed during the post-treatment process (washing and calcination), relatively large pores and large pore volumes could form on the surface of the S-2 particles.

The specific conditions, under which the silicate solution was extracted, affected not only the morphology of the silica particles, but also the efficiency of the particle collection

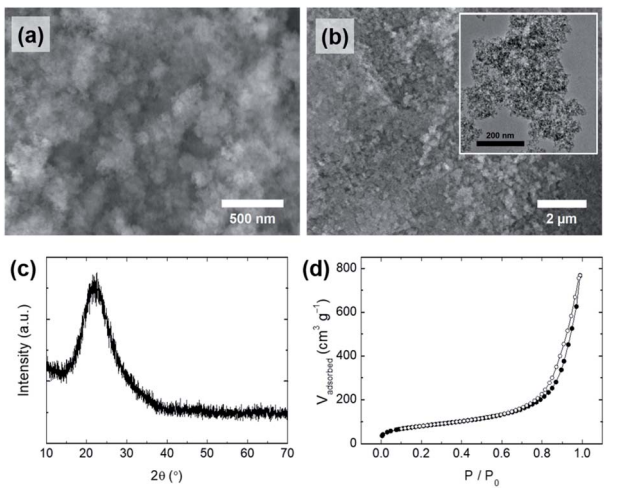

Fig. 5 (a and b) SEM images (inset: TEM image), (c) XRD pattern, and (d) N_2 physisorption isotherms of silica particles (S-2), synthesized using a silicate solution extracted under harsh conditions.

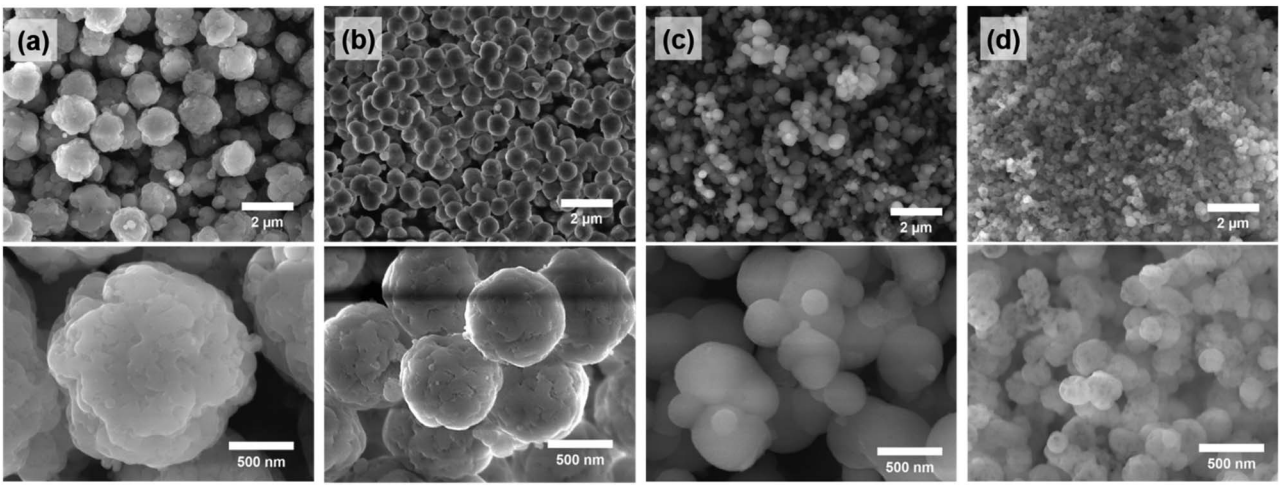

Fig. 6 SEM images of (a) SS-2 (5 °C), (b) SS-1 (25 °C), (c) SS-3 (40 °C), and (d) SS-4 (60 °C). Each value in parentheses represents the temperature of the precipitation process.

process. Fig. S5† shows the filtration process of the SS-1 sample. When 100 mL of distilled water was used in each washing cycle of SS-1, the filtering time was only 8 s, and a rapid colour change of the sample was observed. Although the filtering speed of the S-1 sample was lower than that of the SS-1 (25 s/100 mL) sample, the S-1 sample could be collected by filtration. However, it proved impossible to separate the S-2 sample from the reactant solution because the filtering speed was extremely low. We assume that a large amount of organic components was filtered out along with silica particles, thereby blocking the space between particles and interfering with the penetration of the solvent. Therefore, the S-2 sample was collected and washed *via* centrifugation (5000 rpm for 5 min), which inevitably increased the processing time.

Size-control of spherical silica particles

By adjusting the temperature during the precipitation step, the size of the spherical silica particles could be controlled in the range of hundreds of nanometers to one micrometer. When the temperature was lowered to 5 °C and the precipitation reaction proceeded, the average particle size increased to ~1.4 μm (Fig. 6a and S6a†). On the other hand, as the temperature during the precipitation step increased to 40 °C and 60 °C, the average particle sizes decreased to ~400 nm and ~250 nm, respectively (Fig. 6c, d, S6b and c†). The particle size is closely related to the nucleation rate; as the reaction temperature increased, the nucleation rate also increased.[36,37] Accordingly, a large number of small nuclei were formed at high temperature, and the growth of these nuclei leads to the formation of small-sized particles. This trend corresponds to the result shown in Fig. 6.

The pore sizes of the silica particles also changed depending on the temperature during the precipitation and aging steps (Fig. 7). The SS-2 sample showed type I isotherms, which are observed in the microporous materials. Meanwhile SS-1, SS-3, and SS-4 samples exhibited type IV isotherms typical of mesoporous materials (Fig. 7a). An abrupt increase of adsorption volumes and hysteresis at high P/P_0 indicates the presence of large-sized mesopores. This means that the mesopores of SS-4 exhibit a larger size than SS-1 and SS-3. As the temperature increased from 5 to 60 °C, the main pore size of the silica particles increased from less than 2 nm to approximately 10 nm (Fig. 7b). This tendency is thought to be related to the change in the hydrophilicity of PEG with temperature. An increase in temperature results in the dehydration of EO chains, thereby

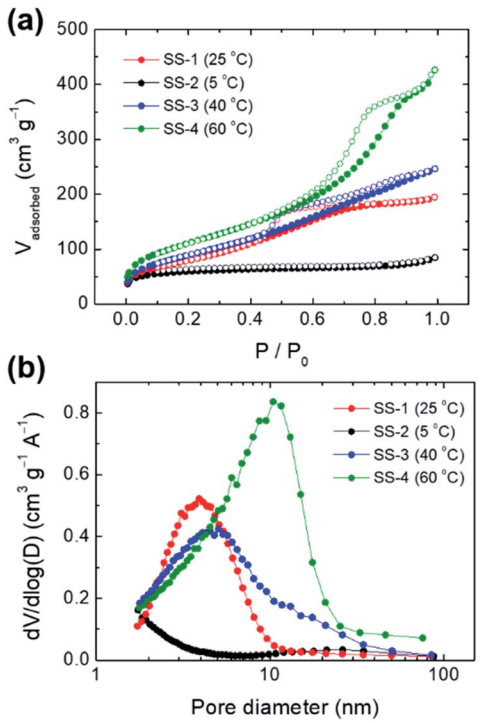

Fig. 7 (a) N_2 physisorption isotherms and (b) pore size distributions of SS-1 (25 °C), SS-2 (5 °C), SS-3 (40 °C), and SS-4 (60 °C). Each value in parentheses represents the temperature of the precipitation process.

decreasing the hydrophilicity of the chains.[38,39] Accordingly, more stretched PEG molecules were confined to the silicate frameworks of SS-2 during precipitation at 5 °C, leading to the formation of micropores (<2 nm). Low hydrophilicity at increased temperature induces large EO–EO aggregates. It weakens the interaction between EO chains and silicates when the PEG and silicate oligomers cooperatively assembled. As a result, the size of the pores generated by the PEG aggregates increased at high temperature (Fig. 7b).

Conclusions

In summary, we developed an eco-friendly and facile method to synthesize size-controlled spherical silica particles from rice husk. Through the alkali extraction of a silicate solution from rice husk under mild conditions followed by precipitation using acetic acid with a PEG additive, morphology-controlled silica was successfully obtained without the use of strong acids and special equipment. The obtained silica particles had a uniformly spherical shape with a high purity and large surface area. We found that the addition of PEG during the precipitation step was important for obtaining spherical silica particles. The use of a silicate solution under appropriate conditions affected not only the morphology of the silica particles, but also the efficiency of particle collection and washing. Additionally, by adjusting the reaction temperature during precipitation, the size of the silica particles could be controlled in the range of ~250 nm to ~1.4 μm. The findings of this study contribute to the development of rice husk-derived silica that can be applied to practical industrial applications.

Experimental section

Materials

Rice husk was obtained from a rice processing facility in the Chungbuk region, Rep. Korea, which was harvested in 2019. It was collected directly from the outlet of the rice husking unit of the milling machine. Rice varieties also influence the properties of silica obtained from rice husk.[40] However, in this study, rice husk obtained from various varieties of rice was used because the rice mill factory from which we obtained the rice husk collected them in the same tank regardless of the variety of rice. Sodium hydroxide powder was purchased from Daejung Chemicals & Metals Inc. (Rep. Korea). It was dissolved in distilled water and used in the experiments. Acetic acid (99.7%, Kanto Chemicals) and PEG (M_r: 2700–3300, Aldrich) were used as received without further purification.

Extraction of silica from rice husks

Rice husk was washed with deionized water three times before use. The washed rice husk was dried at 80 °C overnight. The dried rice husk was immersed in NaOH solution so that the solid content was 6% (w/v). The sample was heated in a heating oven (ThermoStable™ "OF-105", Daihan Scientific Co., Rep. Korea) set at a specific reaction temperature for 3 h. After the reaction, the solution was separated from the solids using vacuum filtration (Circulating Aspirator (WJ-15, SIBATA)) and filter paper (Whatman no. 41, 20–25 μm). To measure the silica extraction yield, acetic acid was added to the solution to adjust the pH to 7.0. The precipitation was thoroughly washed with deionized water and dried at 80 °C overnight, followed by calcining at 900 °C (ramp rate: 5 °C min^{-1}) for 6 h. The silica extraction yield was calculated using eqn (1) below:

$$\text{Silica extraction yield} = \text{weight of ash precipitated/weight of ash in RH} \times 100 \quad (1)$$

Synthesis of spherical silica particles from rice husk-derived silicate solution

In a typical synthesis of SS-1, 0.4 g of PEG was dissolved in 200 mL of the silicate solution at room temperature (25 °C). Then, 5 mL of acetic acid was added to the silicate solution. After stirring overnight at room temperature, the resulting solution was filtered and washed with distilled water. The washed product was then calcined at 550 °C (ramp rate: 2 °C min^{-1}) for 2 h. The overall synthetic procedure for the other SS samples was similar to that of SS-1, except that the reaction temperature was adjusted to 5 °C (SS-2), 40 °C (SS-3), and 60 °C (SS-4), before the addition of acetic acid. The S-1 sample was obtained through the same synthetic procedure as SS-1, with the exception of PEG not being used prior to the addition of acetic acid. The S-1 and SS series samples were synthesized using a silicate solution extracted under mild conditions (80 °C). In contrast, a silicate solution extracted under harsh conditions (150 °C) was used for the synthesis of the S-2 sample. The synthetic method for S-2 was the same as that for SS-1. However, after the addition of acetic acid and further stirring, we were unable to collect the silica product by filtration owing to very slow filtration. For this reason, the silica product was separated by centrifugation at 5000 rpm for 5 min and washed with distilled water several times.

Material characterization

The composition of rice husk was measured according to the standard procedure provided by the National Renewable Energy Laboratory (NREL).[41–43] Briefly, acid hydrolysis was performed with concentrated and diluted sulfuric acid to dissolve cellulose and hemicellulose. The composition of carbohydrate was analysed by using a high-performance liquid chromatograph equipped with a refractive index detector (Agilent 1200, USA). An Aminex HPX-87P column (BioRad, USA) was used. The acid-soluble lignin content was measured *via* UV spectroscopy (V-550 UV-vis spectrophotometer, Japan) at 320 nm. The acid-insoluble lignin and ash contents were determined by burning the samples at 575 °C. A field-emission scanning electron microscope (FE-SEM; JEOL, JSM-7000F, Japan, acceleration voltage: 10.0 kV) and a transmission electron microscope (TEM; JEOL, JEM-2000EX, Japan, acceleration voltage: 200 kV) were used to analyze the material morphologies. SEM images were obtained without additional metal coating. The particle size distributions

of spherical silica were analyzed using ImageJ software on the SEM images. Powder X-ray diffraction (XRD) patterns were obtained using a Bruker D8 Advance (Bruker Corporation, USA) at a scan rate of 6.00° min^{-1}. The nitrogen (N_2) adsorption/desorption isotherms were obtained at 77 K using a Tristar 3020 system (Micromeritics Inc., USA). The samples were degassed at 300 °C for 6 h before measurements. The surface areas were calculated from the measured isotherms according to the Brunauer–Emmett–Teller (BET) method, and the pore volumes were taken at the $P/P_0 = \sim 0.995$ single point. The pore size distributions were calculated by the Barrett–Joyner–Halenda (BJH) method from the adsorption branches of the isotherms. The inorganic composition and carbon content of the silica samples were determined by using an inductively coupled plasma-optical emission spectrometer (ICP-OES; PerkinElmer Inc., Optima 8300 DV, USA) and a CS 744 carbon/sulfur analyzer (LECO Corporation, USA), respectively. Fourier-transform infrared (FTIR) analysis was performed using the attenuated total reflection (ATR) mode on a Nicolet iS 50 FTIR Spectrometer (Thermo Fisher Scientific, USA).

Author contributions

S. Kim: methodology, writing – original draft, and review & editing. J. Y. Park: investigation and visualization. Y. M. Gu: investigation. I. S. Jang: formal analysis. H. Y. Park: formal analysis. K. K. Oh: validation. J. H. Lee: supervision and writing – original draft. J. Chun: conceptualization, writing – original draft, and review & editing.

Conflicts of interest

There are no conflicts to declare.

Acknowledgements

This work was supported by the Korea Institute of Planning and Evaluation for Technology in Food, Agriculture, Forestry (IPET) through the Agro and Livestock Products Safety·Flow Management Technology Development Program, funded by the Ministry of Agriculture, Food and Rural Affairs (MAFRA) (319109-02). This work was further supported by the R&D program of Korea Institute of Energy Technology Evaluation and Planning (KETEP) grant funded by the Ministry of Trade, Industry and Energy (MOTIE), the Republic of Korea (No. 20183030091950).

Notes and references

1 FAOSTAT, available online: http://www.fao.org/faostat/en/data/QC, accessed on 12 November 2020.
2 T. Ding, G. Ma, M. Shui, D. Wan and R. Li, *Chem. Geol.*, 2005, **218**, 41–50.
3 Y. Shen, *Renewable Sustainable Energy Rev.*, 2017, **80**, 453–466.
4 J. Chun, Y. M. Gu, J. Hwang, K. K. Oh and J. H. Lee, *J. Ind. Eng. Chem.*, 2020, **81**, 135–143.
5 I. J. Fernandes, D. Calheiro, A. G. Kieling, C. A. Moraes, T. L. Rocha, F. A. Brehm and R. C. Modolo, *Fuel*, 2016, **165**, 351–359.
6 H. Beidaghy Dizaji, T. Zeng, I. Hartmann, D. Enke, T. Schliermann, V. Lenz and M. Bidabadi, *Appl. Sci.*, 2019, **9**, 1083.
7 T.-H. Liou and C.-C. Yang, *Mater. Sci. Eng., B*, 2011, **176**, 521–529.
8 A. G. Vayghan, A. Khaloo and F. Rajabipour, *Cem. Concr. Compos.*, 2013, **39**, 131–140.
9 J. H. Lee, J. H. Kwon, J.-W. Lee, H.-s. Lee, J. H. Chang and B.-I. Sang, *J. Ind. Eng. Chem.*, 2017, **50**, 79–85.
10 P. Chen, H. Bie and R. Bie, *Korean J. Chem. Eng.*, 2018, **35**, 1911–1918.
11 A. Junpen, J. Pansuk, O. Kamnoet, P. Cheewaphongphan and S. Garivait, *Atmosphere*, 2018, **9**, 449.
12 J. Chun and J. H. Lee, *Sustainability*, 2020, **12**, 10683.
13 X. Ji, S. Evers, R. Black and L. F. Nazar, *Nat. Commun.*, 2011, **2**, 1–7.
14 Y. Wang, Q. Zhao, N. Han, L. Bai, J. Li, J. Liu, E. Che, L. Hu, Q. Zhang and T. Jiang, *Nanomed.*, 2015, **11**, 313–327.
15 J. Liang, Z. Liang, R. Zou and Y. Zhao, *Adv. Mater.*, 2017, **29**, 1701139.
16 N. Z. Knežević, N. a. Ilić, V. Dokić, R. Petrović and D. o. e. Janaćković, *ACS Appl. Mater. Interfaces*, 2018, **10**, 20231–20236.
17 P. Singh and K. Sen, *J. Porous Mater.*, 2018, **25**, 965–987.
18 J. Hwang, S. Kim, U. Wiesner and J. Lee, *Adv. Mater.*, 2018, **30**, 1801127.
19 C. Lim, E.-B. Cho and D. Kim, *Korean J. Chem. Eng.*, 2019, **36**, 166–172.
20 S. Suyanta and A. Kuncaka, *Indones. J. Chem.*, 2011, **11**, 279–284.
21 S. T. Ho, Q. K. Dinh, T. H. Tran, H. P. Nguyen and T. D. Nguyen, *Can. J. Chem. Eng.*, 2013, **91**, 34–46.
22 T. Areerob, N. Grisdanurak and S. Chiarakorn, *Environ. Sci. Pollut. Res.*, 2016, **23**, 5538–5548.
23 S. Kamari and F. Ghorbani, *Environ. Technol.*, 2017, **38**, 1562–1579.
24 B. Purnawira, H. Purwaningsih, Y. Ervianto, V. Pratiwi, D. Susanti, R. Rochiem and A. Purniawan, *IOP Conf. Ser.: Mater. Sci. Eng.*, 2019, **541**, 012018.
25 W. Henao, L. Jaramillo, D. López, M. Romero-Sáez and R. Buitrago-Sierra, *J. Environ. Chem. Eng.*, 2020, **8**, 104362.
26 S. Kamari and F. Ghorbani, *Biomass Convers. Biorefin.*, 2020, DOI: 10.1007/s13399-020-00637-w.
27 R. J. Ramalingam, J. N. Appaturi, T. Pulingam, H. A. Al-Lohedan and D. M. Al-dhayan, *Renewable Energy*, 2020, **160**, 564–574.
28 M. R. AbuKhadra, A. S. Mohamed, A. M. El-Sherbeeny and M. A. Elmeligy, *J. Hazard. Mater.*, 2020, **389**, 122129.
29 N. S. C. Zulkifli, I. Ab Rahman, D. Mohamad and A. Husein, *Ceram. Int.*, 2013, **39**, 4559–4567.
30 C. N. H. Thuc and H. H. Thuc, *Nanoscale Res. Lett.*, 2013, **8**, 1–10.
31 U. Zulfiqar, T. Subhani and S. W. Husain, *J. Non-Cryst. Solids*, 2015, **429**, 61–69.

32 M. Shahnani, M. Mohebbi, A. Mehdi, A. Ghassempour and H. Y. Aboul-Enein, *Ind. Crops Prod.*, 2018, **121**, 236–240.
33 R. Rajan, Y. Zakaria, S. Shamsuddin and N. F. N. Hassan, *Arabian J. Chem.*, 2020, **13**, 8119–8132.
34 K. Kosuge, N. Kikukawa and M. Takemori, *Chem. Mater.*, 2004, **16**, 4181–4186.
35 J. Hwang, J. H. Lee and J. Chun, *Mater. Lett.*, 2021, **283**, 128765.
36 J. W. Yoo, D. S. Yun and H. J. Kim, *J. Nanosci. Nanotechnol.*, 2006, **6**, 3343–3346.
37 I. M. Joni, Rukiah and C. Panatarani, *AIP Conf. Proc.*, 2020, **2219**, 080018.
38 M. Kruk, M. Jaroniec, C. H. Ko and R. Ryoo, *Chem. Mater.*, 2000, **12**, 1961–1968.
39 A. Galarneau, H. Cambon, F. Di Renzo, R. Ryoo, M. Choi and F. Fajula, *New J. Chem.*, 2003, **27**, 73–79.
40 E. Menya, P. W. Olupot, H. Storz, M. Lubwama and Y. Kiros, *Waste Manage.*, 2018, **81**, 104–116.
41 A. Sluiter, B. Hames, R. Ruiz, C. Scarlata, J. Sluiter, D. Templeton and D. Crocker, NREL/TP-510-42618, National Renewable Energy Laboratory, Colorado, 2008.
42 A. Sluiter, R. Ruiz, C. Scarlata, J. Sluiter and D. Templeton, NREL/TP-510-42619, National Renewable Energy Laboratory, Colorado, 2005.
43 A. Sluiter, B. Hames, R. Ruiz, C. Scarlata, J. Sluiter and D. Templeton, NREL/TP-510-42622, National Renewable Energy Laboratory, Colorado, 2005.